Assessing Climatic Control on Erosion Dynamics in Alpine Glacial Cirques: Evidence from the Neoglacial and Younger Dryas Periods

Quentin Portal [1*] , Jean-Francois Buoncristani [2] , Benjamin Pohl [2] , Romain Delunel [3] & Jean-Louis Mugnier[1]

[1] ISTerre, UMR 5275, Univ. Savoie Mont Blanc, Univ. Grenoble Alpes, CNRS, IRD, Univ. Gustave Eiffel, 73370 le Bourget-du-Lac, France

[2] Biogéosciences, UMR/CNRS 6282, Univ. Bourgogne Europe, 6 Bd Gabriel, 21000 Dijon, Univ. Lyon 2, CNRS, UMR 5600 EVS, 69576 Bron, France

[3] Univ. Lyon 2, CNRS, UMR 5600 EVS, 69576 Bron, France

quentin.portal1@univ-smb.fr ; Quentin Portal, 24-28 Av. du Lac d'Annecy, 73370 Le Bourget-du-Lac

jfbuon@u-bourgogne.fr

benjamin.pohl@u-bourgogne.fr

romain.delunel@univ-lyon2.fr

jean-louis.mugnier@univ-smb.fr

Assessing Climatic Control on Erosion Dynamics in Alpine Glacial Cirques: Evidence from the Neoglacial and Younger Dryas Periods – Supplementary

S1 – Data from surface exposure dating using cosmogenic ^{10}Be in the Mont Banc and Gran Paradiso massifs

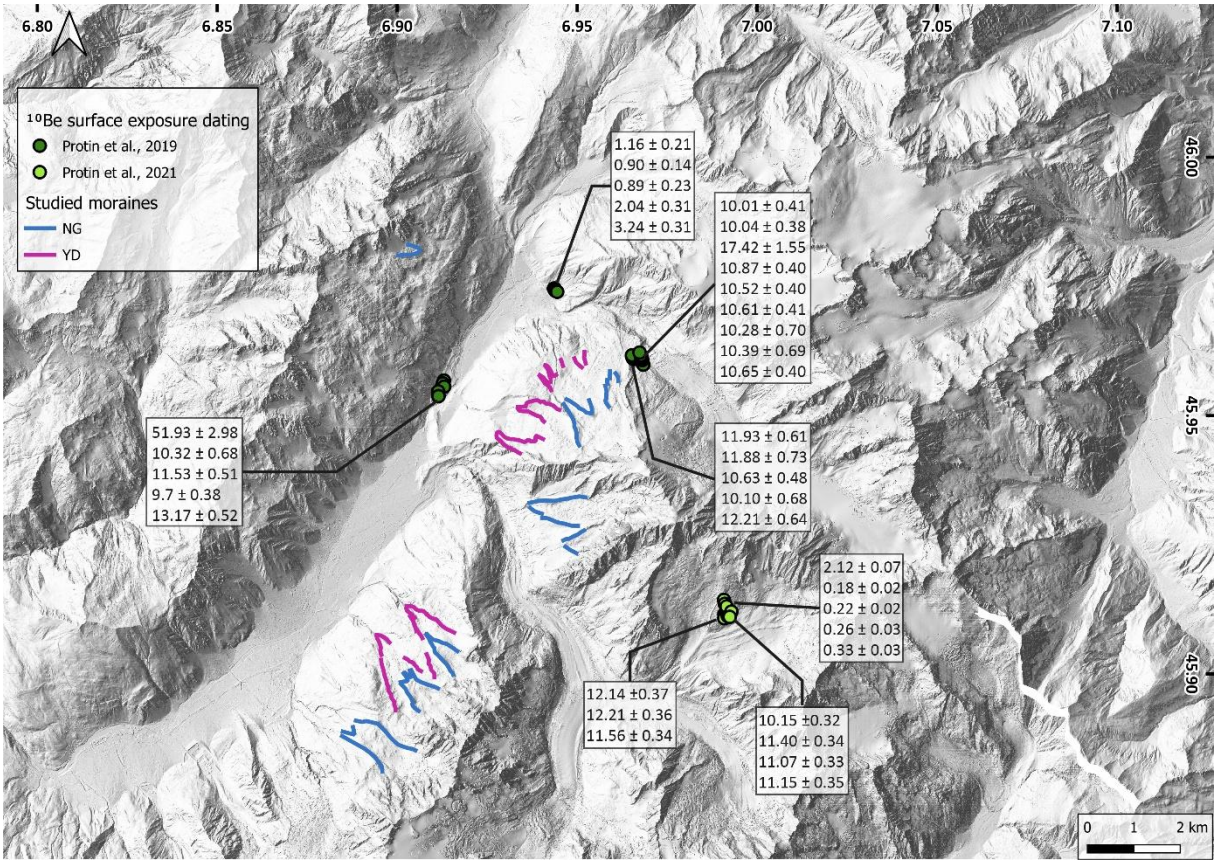

Figure S1-1. ^{10}Be surface exposure dating around the studied moraines of the Mont Blanc massif. Exposure ages are expressed in ka BP.

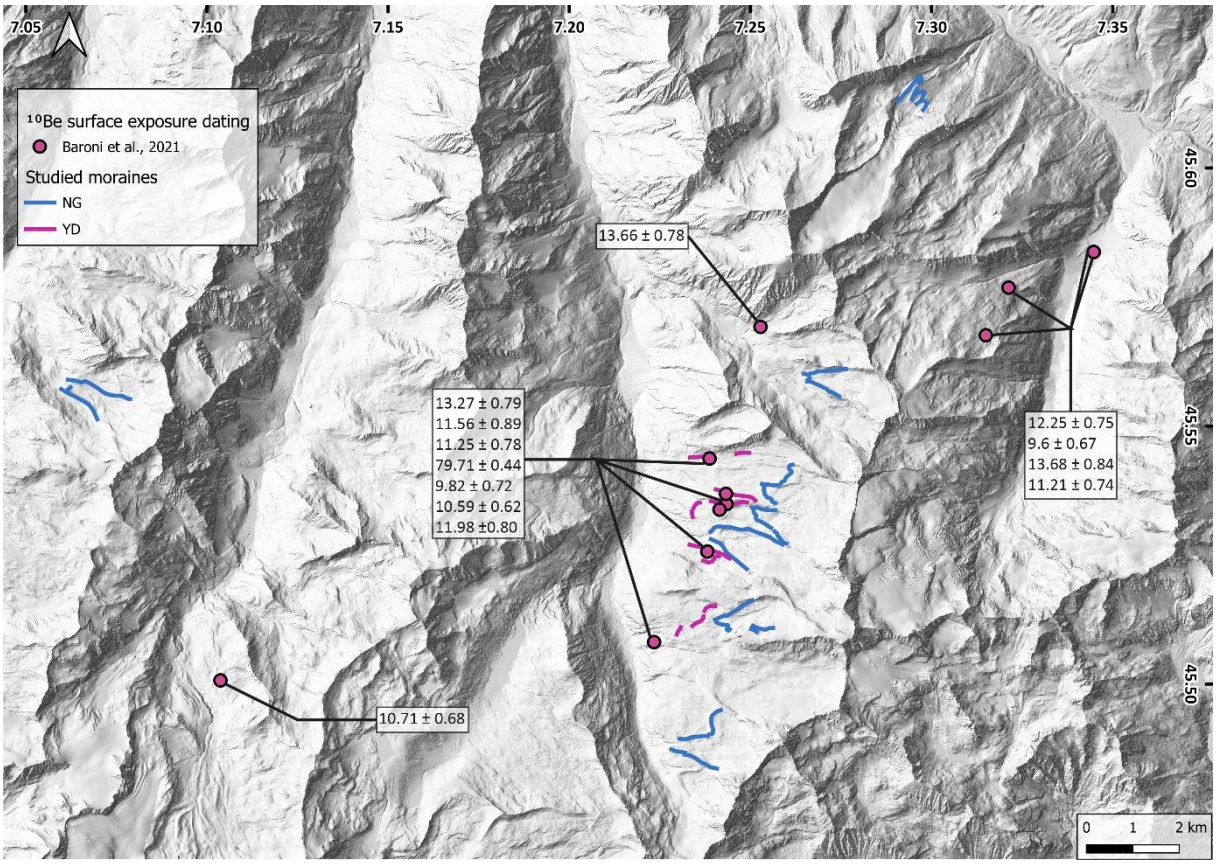

Figure S1-2. ^{10}Be surface exposure dating around the studied moraines of the Gran Paradiso massif. Exposure ages are expressed in ka BP.

S2 – Positive Degree Day glacial model

S2.1 – Climatic parameters

Climatic variables were derived from daily meteorological data collected at French, Italian, and Swiss stations between 1979 and 2014 (Table S1-1). The quality and representativeness of these data were discussed by Joly et al. [2017]. Mean monthly temperatures, their standard deviation, and mean monthly precipitation were calculated for the Mont Blanc and Aiguilles Rouges massifs and for the Gran Paradiso massif from 1979 to 2014, using data from Chamonix-Mont-Blanc and Peisey-Nancroix stations, respectively (Table S1-2). Monthly altitudinal gradients of temperature (Table S1-3) and annual altitudinal gradient of precipitation (Table S1-4) were derived through linear regression across multiple stations. However, the dataset's temporal coverage was constrained due to incomplete annual data from a sufficient number of stations. For the Mont Blanc massif, the monthly altitudinal gradients of temperature were calculated from 7 stations during the years 2001, 2009, 2010, 2011, and 2012, while the annual altitudinal gradient of precipitation was derived from 6 stations between 1994 and 2014. For the Gran Paradiso massif, the monthly altitudinal gradients of temperature were derived from 6 stations between 1985 and 2014, and the altitudinal annual gradient of precipitation was obtained from 6 stations between 1982 and 2014.

Table S2-1. ID, location and altitude of stations used to calculate the climatic parameters of the PDD model. MB = Mont Blanc massif; GP = Gran Paradiso massif; T = Temperature; P = Precipitation.

Station	Location	Latitude (WGS84)	Longitude (WGS84)	Altitude (m)	Massif	Used parameters
74056001	Chamonix-Mont-Blanc	45.92933	6.87738	1044	MB	T, P
74056006	Aiguille du Midi	45.87846	6.88737	3579	MB	T
74085001	Les Contamines	45.82262	6.72807	1158	MB	T, P
74143003	Les Houches	45.89454	6.80094	989	MB	T, P
74256001	Sallanches	45.93196	6.65032	551	MB	T, P
74290002	Vallorcine	46.03005	6.92715	1287	MB	T, P
73040005	Bessans	45.32072	6.99483	1718	GP	T, P
73054001	Bourg-Saint-Maurice	45.61311	6.76274	880	GP	T, P
73181001	Moutiers	45.48501	6.53344	484	GP	T, P
73197001	Peisey-Nancroix	45.54490	6.75598	1323	GP	T, P
73206001	Pralognan-la-Vanoise	45.38608	6.71644	1412	GP	T, P
GSB	Col du Grand Saint-Bernard	45.86998	7.17170	2517	GP, MB	T, P

Table S1-2. Monthly climatic parameters (1979 – 2014 period) used in the PDD glacial model for the Mont Blanc and Aiguilles Rouges massifs (Chamonix-Mont-Blanc's station) and for the Gran Paradiso massif (Peisey-Nancroix's station). MB = Mont Blanc massif; GP = Gran Paradiso massif.

Month	Mean temperature (°C)		Mean temperature standard deviation		Mean precipitation (mm)	
	MB	GP	MB	GP	MB	GP
01 – jan	-2.154	-0.557	2.099	2.204	111.944	85.114
02 – feb	-0.686	0.076	2.409	2.573	96.319	70.392
03 – mar	3.160	3.369	1.890	2.058	94.931	71.344
04 – apr	6.652	6.399	1.683	1.856	87.931	62.989
05 – may	11.111	10.891	1.711	1.839	127.067	88.761

06 – jun	14.398	14.324	1.458	1.701	136.636	92.822
07 – jul	16.379	16.680	1.526	1.720	143.547	81.767
08 – aug	15.964	16.531	1.202	1.627	132.433	76.986
09 – sep	12.712	13.092	1.362	1.774	109.833	76.539
10 – oct	8.734	9.143	1.516	1.758	119.258	87.750
11 – nov	2.790	3.560	1.973	2.132	102.908	81.142
12 – dec	-1.548	-0.143	1.703	1.876	136.667	101.022

Table S1-3. Altitudinal monthly gradients of temperature used in the PDD glacial modelling for the Mont Blanc and Aiguilles Rouges massifs and for the Gran Paradiso massif. MB = Mont Blanc massif; GP = Gran Paradiso massif.

Month	**Altitudinal monthly gradient of temperature (°C.1000m^{-1})**	
	MB (7 stations; years 2001, 2009, 2010, 2011, 2012)	GP (6 stations; 1985 – 2014 period)
01 – jan	4.780	4.862
02 – feb	5.513	5.886
03 – mar	6.304	6.996
04 – apr	6.851	7.376
05 – may	6.853	7.212
06 – jun	6.824	6.745
07 – jul	6.721	6.535
08 – aug	6.334	6.291
09 – sep	6.038	6.066
10 – oct	5.567	5.683
11 – nov	5.068	5.276
12 – dec	5.015	4.549

Table S1-4. Annual altitudinal gradient of precipitation used in the PDD glacial modelling for the Mont Blanc and Aiguilles Rouges massifs and for the Gran Paradiso massif. MB = Mont Blanc massif; GP = Gran Paradiso massif.

Altitudinal annual gradient of precipitation (mm.1000m^{-1})	
MB (6 stations; 1994 – 2014 period)	GP (6 stations; 1982 – 2014 period)
630	600

S2.2 – Positive Degree Day glaciological model

The PDD model used in this study is adapted from the formulation proposed by Harper and Humphrey [2003], further refined by Blard et al. [2007]. In this model, annual accumulation is calculated as the fraction of annual precipitation falling as snow, defined as precipitation occurring when the temperature is below the rain–snow threshold (Equation S1-1).

$$P_{snow} = \frac{P_t}{\sigma\sqrt{2\Pi}} \int_{-\infty}^{T_{rs}} e^{\frac{-(T-T_m)^2}{2\sigma^2}} dT \text{ (Eq. S1-1)}$$

Where P_{snow} represents precipitation occurring as snow in mm.a^{-1}; P_t denotes total precipitation in mm.a^{-1}; σ is the standard deviation of the mean temperature T_m; T_{rs} is the temperature at the rain–snow threshold. Temperatures are expressed in °C.

Annual ablation is calculated by assuming that a certain thickness of snow or ice melts per day and per positive degree, using a Degree Day Factor (DDF). Different DDFs are applied for snow and ice to account for their distinct melt characteristics. Over a given period, if snow ablation is less than accumulation (accumulation zone), then only snow ablation is considered and corresponds to the total ablation (Equation S1-2).

$$A = A_{snow} = 365 \times DDF_{snow} \times T_{PDD} \text{ (Eq. S1-2)}$$

Where A is the annual ablation and A_{snow} is the annual snow ablation in mm.a^{-1}; DDF_{snow} is the snow melt factor in mm.day^{-1}.°C^{-1}; T_{PDD} is the integrated positive annual temperature in °C.

Conversely, if snow ablation exceeds accumulation (ablation zone), then total ablation corresponds to the sum of snow ablation (equivalent to total accumulation) and ice ablation (Equation S1-3).

$$A = A_{snow} + A_{ice} = S + 365 \times DDF_{ice} \times T_{PDD} \text{ (Eq. S1-3)}$$

Where A is the annual ablation and A_{snow} is the annual snow ablation and A_{ice} is the annual ice ablation in mm.a^{-1}; DDF_{snow} is the snow melt factor in mm.day^{-1}.°C^{-1}; T_{PDD} is the integrated positive annual temperature in °C.

Integrated positive temperature is calculated from the mean temperature and its standard deviation (Equation S1-4).

$$T_{PDD} = \frac{1}{\sigma\sqrt{2\Pi}} \int_{0}^{+\infty} T e^{\frac{-(T-T_m)^2}{2\sigma^2}} dT \text{ (Eq. S1-4)}$$

Where T_{PDD} is the integrated positive annual temperature and T_m is the mean temperature in °C; σ is the standard deviation of T_m.

Glacier sliding on the topography is defined by a threshold of basal shear stress of ice on bedrock. A value of 1 bar is conventionally used to represent an equilibrium glacier [Paterson, 1994; Harper and Humphrey, 2003]. The thickness of ice that can accumulate on a topographic grid cell before exceeding the basal shear threshold decreases with slope (Equation S1-5).

To improve the model's realism, a stability threshold was introduced for slopes of 35° and more, beyond which accumulated snow fully slides onto underlying areas. This adjustment prevents the unrealistic formation of excessive ice on steep walls, which is a limitation of the original model.

$$H = \frac{\tau}{\rho \times g \times sin\,(\alpha)} \text{ (Eq. S1-5)}$$

Where H is the ice thickness in meters; τ is the basal shear stress in Pa; ρ is the ice density in kg.m^{-3}; g is gravitational acceleration in m.s^{-2}; and α is the slope in degrees.

S2.3 – Glaciological parameters

Degree Day Factors (DDF) for snow and ice were derived from values calculated in several studies on the Argentiere and Mer de Glace glaciers, both located on the northern face of the Mont Blanc massif. The DDF values used in this study are 3.3 mm.day^{-1}.°C^{-1} for snow and 5.4 mm.day^{-1}.°C^{-1} for ice, representing the average of those calculated in the cited studies (Table S1-5).

Table S1-5. Degree Day Factor (DDF) values for snow and ice calculated on the Argentière and Mer de Glace glaciers, along with the obtained averages.

Glacier	**DDF$_{snow}$ (mm.day^{-1}.°C^{-1})**	**DDF$_{ice}$ (mm.day^{-1}.°C^{-1})**	**Study**
Argentiere	3	6.1	Six and Vincent, 2014
Argentiere	3.5	5.5	Réveillet et al., 2017
Mer de Glace	4.4	4.8	Réveillet et al., 2017
Argentière	2.3	5.1	Protin et al., 2019
Mean	**3.3**	**5.4**	**This study**

S3 – DEM data

The LiDAR Digital Elevation Models (DEMs) used in this study are as follows:

- France: 1 m resolution DEM interpolated from *LiDAR HD* data https://geoservices.ign.fr/lidarhd
- Italy: 2 m resolution DEM from *DTM 2005/2008* https://mappe.partout.it/pub/geonavitg/geodownload.asp?carta=DTM0508
- Switzerland: 0.5 m resolution DEM from *SwissALTI3D* https://www.swisstopo.admin.ch/fr/modele-altimetrique-swissalti3d

S4 – Error estimation of moraine volume calculation

Comparison between the real polished bedrock surface and the "thin plate spline" interpolation [Donato and Belongie, 2002] used in this study (Figure S3-1) to assess the accuracy of the volume calculation method. Thin plate spline is an algorithm developed to create smooth interpolation using scattered data, including topographic modelling.

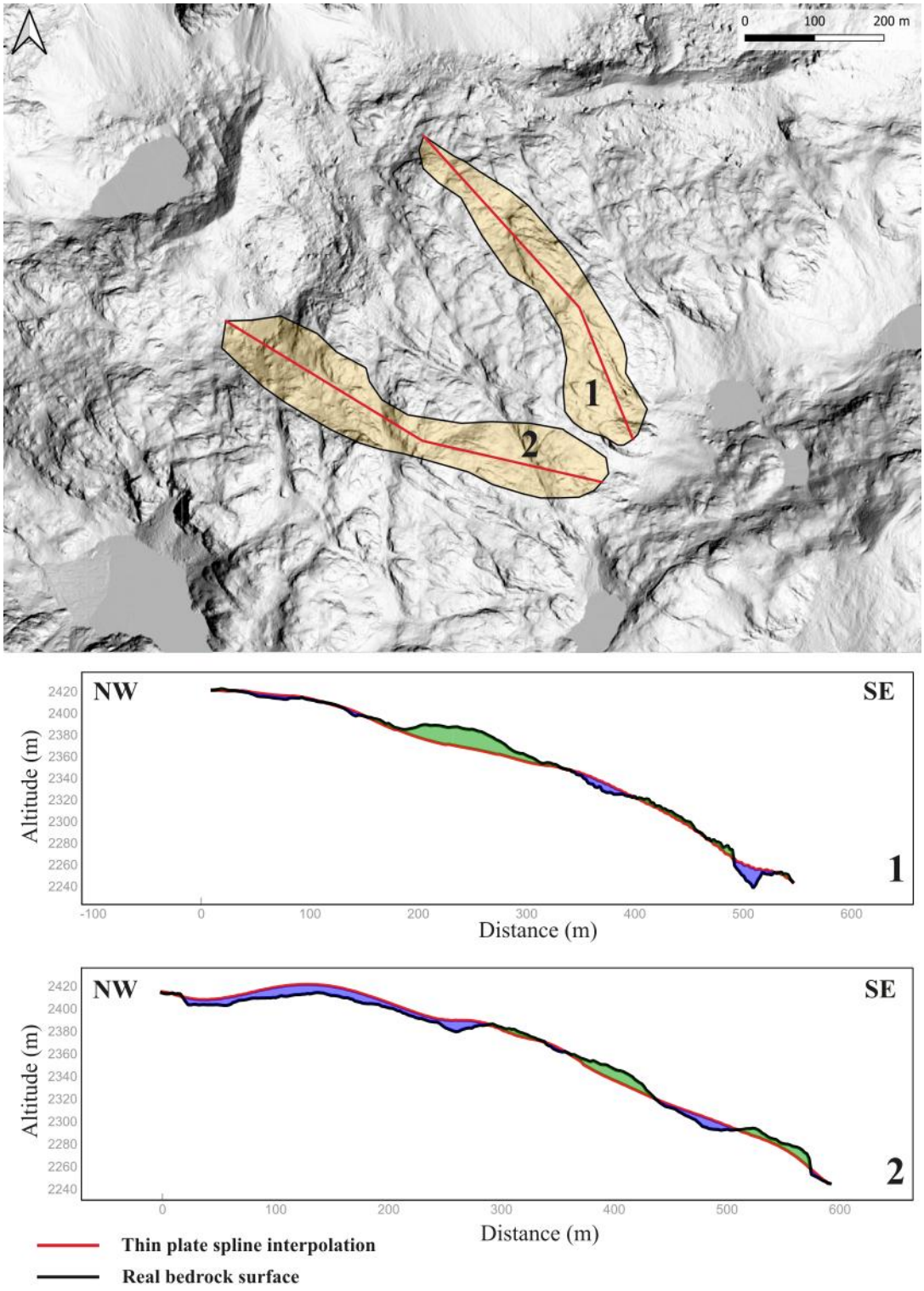

Figure S4-1. Artificial cirque moraine-like surface (yellow) on polished bedrock in the Aiguilles Rouges massif, where the thin plate spline surface interpolation was applied. (1)

Cross-section in the northern surface; (2) Cross-section in the southern surface. The volume discrepancy between the interpolated surface and the real topography is approximately 7 %, with excess volumes shown in blue and deficit volumes in green.

S5 – Paleoclimatic and geomorphological parameters of cirques

The climatic parameters obtained for the YD and NG applying the PDD modelling climate calibration to the CHELSA spatial database [Karger et al., 2017] for each studied cirque are detailed in Table S4-1. Geomorphological parameters (Table S4-2) are provided only for the NG, as they were not used for the YD.

Table S5-1. Detailed climatological parameters of the studied glacial cirques. MB = Mont Blanc; AR = Aiguilles Rouges; GP = Gran Paradiso; NG = Neoglacial; YD = Younger Dryas.

Glacial cirque (massif)	Period	Mean annual temperature (°C)	Mean annual precipitation ($kg.m^{-2}.an^{-1}$)
Nant Blanc (MB)	NG	-5.78	2640
Nantillons (MB)	NG	-4.12	2670
Blaitière (MB)	NG	-4.69	2758
Nantillons et Blaitière (MB)	YD	-6.57	1096
Pèlerins (MB)	NG	-5.38	2912
Drus (MB)	NG	-4.19	2527
Pendant and Lognan (MB)	NG	-4.41	2698
Pendant and Lognan (MB)	YD	-6.14	1099
Remuaz (AR)	NG	-2.88	3277
Gran Paradiso (GP)	NG	-6.39	2144
Gran Paradiso (GP)	YD	-9.20	853
Monciair (GP)	NG	-5.27	2121
Trajo (GP)	NG	-6.54	2285
Invergnan (GP)	NG	-5.64	2368
Timorion (GP)	NG	-6.37	2322

Table S5-2. Detailed geomorphological parameters of the studied glacial cirques.

Glacial cirque (massif)	Surface area (km^2)	Min altitude (m)	Max altitude (m)	Mean altitude (m)	Relief (m)	Median slope (°)
Nant Blanc (MB)	4.39	1890	4102	2890	2212	36.6
Nantillons (MB)	1.94	2087	3506	2768	1419	39.6
Blaitière (MB)	2.74	2147	3636	2720	1489	37.1

Pèlerins (MB)	6.04	1766	3821	2816	2055	44.4
Drus (MB)	1.52	2102	3714	2725	1612	49.3
Pendant and Lognan (MB)	2.49	2194	3400	2707	1206	27.1
Remuaz (AR)	0.59	2302	2900	2552	598	35.0
Gran Paradiso (GP)	9.44	2503	4057	3242	1554	25.0
Monciair (GP)	2.19	2618	3629	3001	1011	24.0
Trajo (GP)	5.10	2206	3969	3175	1763	25.4
Invergnan (GP)	2.02	2531	3572	3007	1041	32.2
Timorion (GP)	1.47	2739	3546	3178	807	22.2

S6 - Compilation of erosion data of glacial cirques

The compiled data used in Section 5.1 are presented in Table S5-1, which also includes moraine volumes.

Table S6-1. Compilation of erosion data in NG glacial cirques based on moraine volumes.

Glacial cirque	Region	Surface area (km^2)	Moraine volume (10^6 m^3)	Denudation rate ($mm.an^{-1}$)	Study
Nant Blanc	Alps	4.39	5.22	0.18	This study
Nantillons	Alps	1.94	5.81	0.45	This study
Blaitière	Alps	2.74	3.72	0.20	This study
Pèlerins	Alps	6.04	7.62	0.19	This study
Drus	Alps	1.52	1.35	0.13	This study
Pendant and Lognan	Alps	2.49	4.51	0.27	This study
Remuaz	Alps	0.59	1.69	0.43	This study
Gran Paradiso	Alps	9.44	12.95	0.21	This study
Monciair	Alps	2.19	4.54	0.31	This study
Trajo	Alps	5.10	4.00	0.12	This study
Invergnan	Alps	2.02	4.06	0.30	This study
Timorion	Alps	1.47	2.39	0.24	This study
C-16	Canadian Arctique	3.14	0.85	0.011	Anderson, 1978
C-18	Canadian Arctique	2.85	2.40	0.027	Anderson, 1978
D-121	Canadian Arctique	2.44	0.41	0.017	Anderson, 1978
D-124	Canadian Arctique	5.50	4.71	0.028	Anderson, 1978
D-128-129	Canadian Arctique	2.66	4.01	0.036	Anderson, 1978
D-135	Canadian Arctique	2.88	0.64	0.011	Anderson, 1978
D-136	Canadian Arctique	5.49	4.05	0.023	Anderson, 1978
D-137	Canadian Arctique	2.04	7.10	0.065	Anderson, 1978
D-138	Canadian Arctique	4.30	3.86	0.026	Anderson, 1978
Maladeta	Pyrenees	1.48	2.53	0.52	Crest, 2017
Aneto	Pyrenees	2.77	1.67	0.18	Crest, 2017

Barrancs	Pyrenees	0.71	0.75	0.32	Crest, 2017
Tempestades	Pyrenees	1.07	1.06	0.30	Crest, 2017
Salenques	Pyrenees	0.80	1.59	0.61	Crest, 2017
Creguenya	Pyrenees	0.25	1.09	1.35	Crest, 2017
Corones	Pyrenees	0.63	0.78	0.38	Crest, 2017
Lloses	Pyrenees	0.51	1.16	0.69	Crest, 2017
Arapaho	Rockies	0.52	0.97	1.65	Reheis, 1975

References

Anderson, L.W., 1978. Cirque Glacier Erosion Rates and Characteristics of Neoglacial Tills, Pangnirtung Fiord Area, Baffin Island, N.W.T., Canada. Arct. Alp. Res. 10, 749. https://doi.org/10.2307/1550741

Baroni, C., Gennaro, S., Salvatore, M.C., Ivy-Ochs, S., Christl, M., Cerrato, R., Orombelli, G., 2021. Last Lateglacial glacier advance in the Gran Paradiso Group reveals relatively drier climatic conditions established in the Western Alps since at least the Younger Dryas. Quat. Sci. Rev. 255, 106815. https://doi.org/10.1016/j.quascirev.2021.106815

Blard, P.H., Lavé, J., Pik, R., Wagnon, P., Bourlès, D., 2007. Persistence of full glacial conditions in the central Pacific until 15,000 years ago. Nature 449, 591–4. https://doi.org/10.1038/nature06142

Crest, Y., 2017. Quantification de la dénudation glaciaire et postglaciaire dans l'orogène pyrénéen : bilans comparés parmi des cirques et des petits bassins versants en contexte climatique océanique et méditerranéen à l'aide des nucléides cosmogéniques produits in-situ et de mesures topométriques sous SIG (phdthesis). Université de Perpignan.

Harper, J., Humphrey, N., 2003. High altitude Himalayan climate inferred from glacial ice flux. Geophys. Res. Lett. 30, 1764. https://doi.org/10.1029/2003GL017329

Joly, D., Berger, A., Buoncristiani, J.-F., Champagne, O., Pergaud, J., Richard, Y., Soare, P., Pohl, B., 2017. Geomatic downscaling of temperatures in the Mont Blanc massif. International Journal of Climatology. https://doi.org/10.1002/joc.5300

Karger, D.N., Conrad, O., Böhner, J., Kawohl, T., Kreft, H., Soria-Auza, R.W., Zimmermann, N.E., Linder, H.P., Kessler, M., 2017. Climatologies at high resolution for the earth's land surface areas. Sci. Data 4, 170122. https://doi.org/10.1038/sdata.2017.122

Paterson, W.S.B., 1994. Physics of Glaciers. Butterworth-Heinemann.

Protin, M., Schimmelpfennig, I., Mugnier, J.-L., Ravanel, L., Le Roy, M., Deline, P., Favier, V., Buoncristiani, J.-F., Aumaître, G., Bourlès, D.L., Keddadouche, K., 2019. Climatic reconstruction for the Younger Dryas/Early Holocene transition and the Little Ice Age based on paleo-extents of Argentière glacier (French Alps). Quat. Sci. Rev. 221, 105863. https://doi.org/10.1016/j.quascirev.2019.105863

Protin, M., Schimmelpfennig, I., Mugnier, J.-L., Buoncristiani, J.-F., Le roy, M., Pohl, B., Moreau, L., 2021. Millennial-scale deglaciation across the European Alps at the transition between the Younger Dryas and the Early Holocene – evidence from a new cosmogenic nuclide chronology. Boreas 50, 671–685. https://doi.org/10.1111/bor.12519

Reheis, M.J., 1975. Source, Transportation and Deposition of Debris on Arapaho Glacier, Front Range, Colorado, U.S.A. J. Glaciol. 14, 407–420. https://doi.org/10.3189/S0022143000021936

Réveillet, M., Vincent, C., Six, D., Rabatel, A., 2017. Which empirical model is best suited to simulate glacier mass balances? J. Glaciol. 63, 39–54. https://doi.org/10.1017/jog.2016.110

Six, D., Vincent, C., 2014. Sensitivity of mass balance and equilibrium-line altitude to climate change in the French Alps. J. Glaciol. 60, 867–878. https://doi.org/10.3189/2014JoG14J014